NUMERICAL INVESTIGATION OF SUPPORT DOMAIN COEFFICIENT OF MOVING LEAST SQUARES SHAPE FUNCTIONS WITH ELEMENT FREE GALERKIN METHOD

[1]SAMET CALISKAN, [2]SAMI KARADENIZ

[1]Odelo Automotive Signal Systems R&D Center Turkey
[2]Mechanical Engineering Department Baskent University Turkey
E - mail: [1]samet.caliskan@odelo.com.tr, [2]samikdeniz@hotmail.com

Abstract - In this paper, the effects of the specific value of the domain radius and the integration cell distributions on the convergence behaviour of the element free Galerkin meshless method are numerically investigated. In the numerical analyses, moving least squares approximation was utilized to construct the mesh free shape functions. Gauss quadrature was chosen as the integration scheme. The back cell integration domains were built for both the bounding box and manual definition methods. To satisfy the Kronecker delta property, the shape functions were modified. The numerical results are compared with the existing analytical and numerical data.

Keywords - Element Free Galerkin Method, Boundary Value Problems, Initial Boundary Value Problems, Moving Least Squares, Domain Radius.

I. INTRODUCTION

In mathematical modelling of a physical phenomenon, in nature, it is a common practice to utilize, differential or integral equations relating various quantities of interest. This is due to the fact that there exist several numerical methods to solve these equations. Among these, the finite difference method (FDM), the finite element method (FEM) and the boundary element method (BEM) are the frequently used for the numerical analysis of the mathematical model. In the first two methods, a set of discrete nodes is defined in the solution domain. These nodes are connected to form a grid or element structure at the beginning of the solution phase to satisfy connectivity condition in solution domain. Mesh free methods, however, use only nodes in the solution of partial differential equations and do not need any element structure to achieve the connectivity. Therefore, in contrast to the conventional numerical methods such as the finite difference and finite element methods, this method eases the mesh generation part of the solution process since no element is required in the entire model. Hence, this methods require no skilled person to build a mesh structure.

In this study the Element Free Galerkin Method (EFGM) is utilized. The EFGM is originally a modified version of the Diffuse Element Method (DEM) developed by Nayroles et al. [1]. In the Diffuse Element Method, an approximation is achieved by replacing the FEM interpolation with a local weighted least squares approximation which is valid within a small neighborhood of the independent variable. However, the DEM suffers a drawback in calculating the derivatives of the local approximations. Here, the local polynomial basis is chosen as differentiable and all other approximations are constants. In EFGM all these terms are considered as differentiable and hence the derivatives can be calculated properly. In addition, the essential boundary conditions are applied very easily for the solution at the nodal points. [1, 2].

The EFG Method was originally developed by Belytschko et al [3]. This method is considered as meshless since it uses only the nodes in the approximation. However, the EFG Method requires a back cell structure for the numerical integrations. The back cell structure is also used for several other purposes; namely at first it helps to identify the local neighbor nodes contributing to the quality of approximation and it also provides a structure to evaluate the integrals with a numerical integration scheme such as Gauss quadrature [4-6]. The cell structures for numerical integration can either be defined manually by selecting a desired number of integration cells in the solution domain or by utilizing, so called, the Bounding Box Method developed by Belytschko et al [4]. The Bounding Box Method is an automatic method to define the cell structure utilized in predicting the intersection of the support domains of the shape functions defined in the solution domain [4]. Defining the back cell structure manually for numerical integration eases the construction process of the integration cells. However, insufficiency in the selection of the integration cells may result in poor approximations. On the other hand, employment of a very large number of nodes, i.e. dense back cells, in the solution domain may cause unnecessarily increases in the solution time. Therefore, a qualified person is required to decide on the sufficiency of the integration cell distribution and density of it. In the bounding box method, however, the selection of the desired number of cells and their locations are an automatic process. Thus, it reduces the need of a

qualified person in the process of the construction of the cell structure. In this method, all the nodes are utilized to define intersections of the shape functions and every intersection of the shape functions will construct the boundary of the back cell structure. The larger the number of shape functions the more complex the cell structure definition becomes. Even with a predefined shape function domain radius, the automatic definition in the bounding box method requires a search process to find possible intersections and to create the integration cells, since the total number of cells cannot be predicted at the beginning of the integration phase. In addition, in meshless methods shape functions are all created during the approximation phase of the partial differential equations. This means a predefined shape function is not present as the moving nature of the Moving Least Squares (MLS) approximation which was utilized in the construction of the meshless shape functions. One another issue in using moving least squares approximation in EFG Method is that the shape functions do not possess the Kronecker delta property. This means that applying the boundary conditions in the meshless methods an alternative approaches such as the Lagrange multipliers, the Singular Value Decomposition or the Penalty Method must be employed. In this study an alternative approach developed by Atluri et al [7] is utilized for applying the boundary conditions as it is in the finite element method where the shape functions possess the Kronecker delta property. In this approach the meshless shape functions are all transformed from satisfying actual nodal values to satisfying fictitious nodal values so that they all possess the Kronecker delta property.

The shape functions in meshless methods are nonzero in the support domain defined by the effective support domain radius and they are zero in the rest of the solution domain. The effectiveness of the shape functions in mesh free methods becomes apparent during the inversion of the Moment matrix. The inverse of the moment matrix is achieved by well posed shape functions which requires at least m+1 shape functions that have a nonzero value on a node in the solution domain for a mth order approximation [2, 8]. This fact controls the effective support domain radius value for the shape functions constructed with the MLS.

To create a fully automated solution procedure for a mesh free method, prediction of the effective support domain coefficient for the MLS shape functions constructed by utilizing spline type weight functions is an important issue. Therefore, decision making in the numerical simulation phase of the analysis is a complex and a knowledge based procedure. If any person, without sufficient skill and knowledge for fulfilling the necessary information for an accurate and well approximated numerical simulation may make wrong or not realistic decisions and assumptions. As a consequence of this the erroneous results may occur which may cause irreversible failures. In such a situation possible mistakes can be avoided by automating the numerical simulation process and thus in this stage of the analysis the need for an experienced and qualified person is eliminated.

In this study the effects of a value the coefficient for effective support domain radius on the numerical solutions obtained by the EFG method is studied. For this purpose the EFG Method is applied to predict the numerical solutions of two transient heat transfer problems and a membrane vibration problem. In the solutions of all these problems the MLS shape functions possessing C0 continuity is employed. The numerical results are compared with the analytical solutions and the numerical predictions obtained by the means of other numerical methods such as the FEM.

II. DETAILS OF NUMERICAL EXPERIMENTATION

2.1. Element Free Galerkin Method

The Element Free Galerkin Method (EFGM) is an alternative meshless approach to the finite element method in the numerical solution of the engineering problems represented by differential equations. The residual form of a differential equation is weighted with the shape functions which are utilized for the approximation of the field variables.

Discretization of the differential equation with the EFGM follows the same procedure as it is in FEM. Hence, a step by step EFGM discretization will be used to solve the 1-D boundary value problems represented by Eq.1.

$$-\frac{d}{dx}\left(\alpha(x)\frac{du(x)}{dx}\right)+\beta(x)u(x)=f(x) \quad (1)$$

Here, $\alpha(x)$ and $\beta(x)$ are material constants and differ for the physical problem that a differential equation refers to.

Discretization procedure of the differential equation is the same as it is in the FEM. The only difference is in the shape functions. Here the weighting functions which employed in weighting the residual equation are all defined with the moving least squares approximation.To produce interpolations for numerical solution algorithms such as meshless methods, the moving least squares method is an alternative approach to least squares approximation with varying weighting function in the support domain of the interpolant. Moving the least squares approach defined in Fig. 1, is a weighted least squares norm between the actual nodal values and approximation $u^h(x)$ in the solution domain. Then a minimization process is performed over the undetermined coefficients in the moving weighted least squares norm [8].

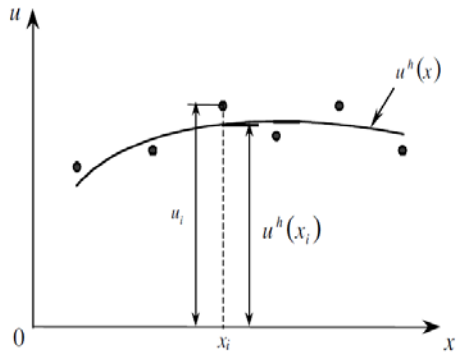


Fig.1. Moving Least Squares Approximation [7]

The moving least square approximation to u over domain, $u^h(x)$ is;

$$u^h(x) = \sum_i^m p_i(x)a_i(x) \qquad (2)$$

In Eq.2m, $p_i(x)$ and a(x) denote number of nodes to be defined in the solution domain, linearly independent basis functions and undetermined coefficients of the approximation, respectively [8, 9]. Applying this minimization procedure results in a set of equations expressed in a compact form in Eq. 3

$$A(x)a(x) = B(x)\{u\} \qquad (3)$$

where, A(x) is the weighted moment matrix of the approximation; Here A(x) and B(x) are given as

$$A(x) = P^T(x)\lambda(x)P(x)$$
$$B(x) = P^T(x)\lambda(x) \qquad (4)$$

where$\lambda(x)$ is the weighting function utilized in the moving least squares approach.In this study spline type weighting functions of the fourth order are employed. The spline type weighting function of the fourth order is defined in Eq. 5.

$$\lambda(s) = 1 - 6s^2 + 8s^3 - 3s^4 \text{ if } s\leq 1$$

$$\lambda(s) = 0 \qquad s>1 \qquad (5)$$

The basis functions are given as

$$P(x) = [1\ x]$$
$$P(x) = [1\ x\ x^2] \qquad (6)$$

In Eq. 6 represents linear and quadratic basis functions. In Eq. 7 meshless shape functions generated with the moving least squares approach are defined. Actual nodal values in Eq. 7 are u_i and ϕ_i the meshless shape functions.

$$u^h(x) = \sum_i^m \phi_i u_i = P^T(x)A^{-1}(x)B(x)u_i \qquad (7)$$
$$\phi_i(x) = \sum_i^m P^T(x)A^{-1}(x)B(x) \qquad (8)$$

The meshless shape functions defined in Eq. 8 do not possess Kronecker delta property. In order to apply the boundary conditions as it is in traditional methods, a transformation of the shape functions ought to be carried out. Atluri et al [7] proposed such a method to transform the shape functions so that the shape functions satisfy the Kronecker Delta property. The transformation of the shape functions illustrated in Fig. 2 [7].

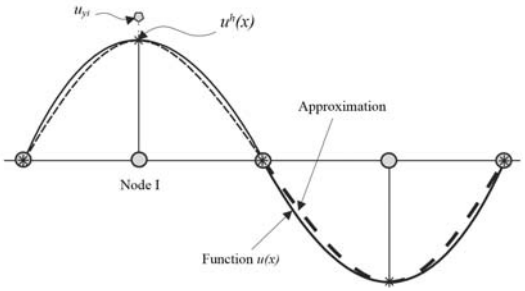


Fig.2 Transformation of the moving least squares shape functions

In this approach, the moving least squares shape functions are represented in terms of fictitious nodal values u_{yi} rather than the local approximation values $u^h(x)$. Thisprocessresults in a properly defined transformation matrix with appropriate coefficients so that new shape functions which satisfy the Kronecker delta property are obtained. The transformation from the local approximation values to the fictitious nodal values are is given in Eq. 9.

$$u^h(x) = \sum_{i=1}^m \phi_i u_{yi} \qquad (9)$$

Reinterpreting the new approximation values in Eq. 9 as local values at a certain node j then the transformation can easily be implemented as

$$u_j = \sum_{i=1}^m \phi_i(x_j)u_{yi} \qquad (10)$$

The fictitious nodal values can be identified in terms of the approximation values given in Eq. 11.

$$u_{yi} = T_{ij}u_j$$
$$T_{ij} = \left[\phi_j(x_i)\right]^{-1} \qquad (11)$$

The transformation matrix can now be defined in terms of the approximation values and the fictitious nodal values. Substituting the transformed fictitious nodal values predicted in Eq. 11 into Eq. 9 a new approximation and transformed moving least squares shape functions can be interpreted clearly.

$$u^h(x) = \sum_{i=1}^m \phi_i(x)\left[\phi_j(x_i)\right]^{-1}u_j \qquad (12)$$

This transformation method was applied to one dimensional moving least squares shape functions in domain size of [0,1] with 7 shape functions having 0.5 support domain radius.

III. RESULTS AND DISCUSSION

The Element Free Galerkin Method is applied for generating the numerical solutions of the problems of the transient heat transfer and a transverse vibration of membrane.

The solution domain and the boundary conditions of the heat transfer problem considered is shown in Fig. 3 [10]. In the solution, the effects of the specified shape function in solution domain, effects of numerical integration and coefficient of support domain of the shape functions are investigated.

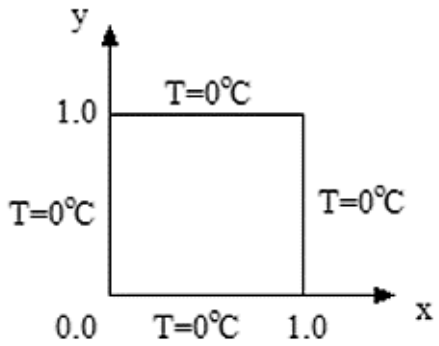


Fig. 3. The heat transfer problem; the domain and boundary conditions

The partial differential equation for the problem is given by Eq. 13.

$$\frac{\partial T}{\partial t} = \frac{1}{\pi^2}\left(\frac{\partial^2 T}{\partial x^2} + \frac{\partial^2 T}{\partial y^2}\right) \qquad (13)$$

The analytical solution to this problem is given by Eq. 14 and illustrated in Fig. 4 at t=2 seconds [10].

$$T(x,y,t) = \frac{1280}{\pi}\left(\sum_{k=0}^{\infty}\sum_{l=0}^{\infty}\frac{\sin(2k+1)\pi x \sin(2l+1)\pi y}{(2l+1)(2k+1)} e^{-\lambda^2(2l+1)(2k+1)}\right) \qquad (14)$$

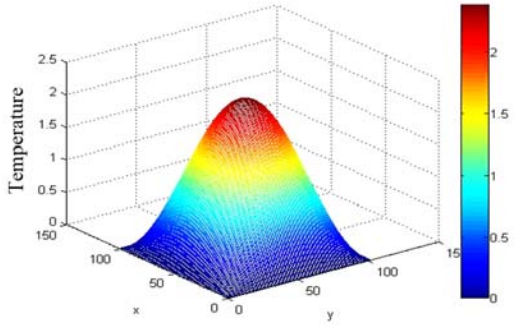


Fig. 4. The analytical solution of the heat transfer problem at t=2 s.

The Element Free Galerkin approximation to this problem are investigated for 7x5 and 11x7 node definitions in x and y axes, respectively. The support domain width is chosen to be 2.35 times the space between two adjacent nodes where a uniform nodal distribution is defined in the solution. Unless otherwise stated the support domain coefficient for the moving least squares shape functions will be 2.35 throughout this analysis. Initial condition for the heat transfer problem $T(x,y,0)=80^0C$ was chosen.. Temperature distributions of the EFG approximations for 7x5 and 11x7 node definitions are shown in Figs. 5 and 6, respectively.

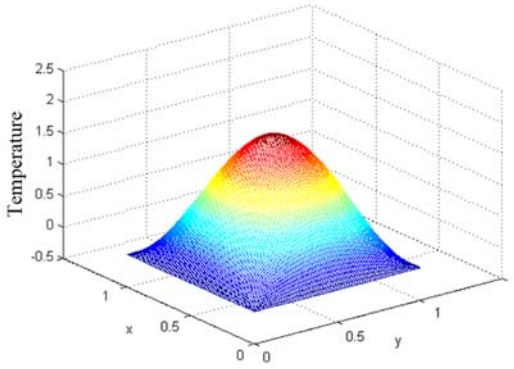


Fig. 5. Element free Galerkin solution of the temperature distribution with a 7x5 node resolution

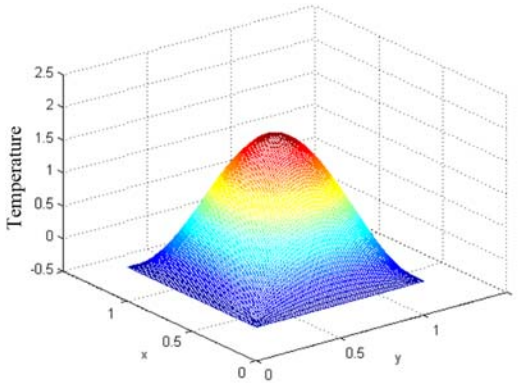


Fig. 6. Element free Galerkin solution of the temperature distribution with a 11x7 node resolution

Comparison of the centerline temperature distributions corresponding to the analytical solution and the EFG solutions with 7x5 and 11x7 node resolutions are illustrated in Fig. 7.

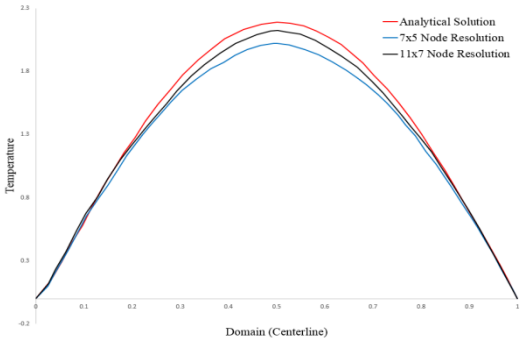


Fig. 7. Comparison of the centerline temperature distributions

As it is seen, increasing the number of nodes in the solution domain results in a more accurate approximation. This is an expected result from a numerical analysis approach as it is the case in the

finite element method. For this problem, the effect of increasing the number of nodes employed in solution domain on the convergence behavior is investigated by carrying out a number of EFG meshless approximations to the illustrative problem. The results are compared with the analytical prediction and illustrated in Fig. 8.

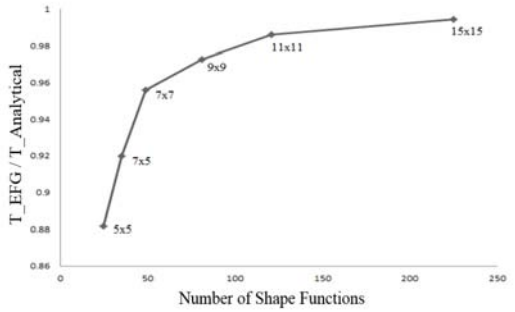


Fig. 8. Effect of number of shape functions on the convergence of the EFG solutions

In these simulations the bounding box method was employed in the evaluation of the integration cells. This technique, as mentioned earlier, was originally proposed by Belytschko et al and was used to define the integration cells by utilizing support domain radius for each node in the solution domain. The support domain of the moving least square shape functions can be defined as the domain of the shape functions with nonzero values. One of the advantages of the bounding box method is that, no experience is needed to decide on the required number of integration cells for generating a sufficiently accurate approximation. Its only disadvantage is that to generate an optimal number of integration cells is not possible. Despite of this deficiency the bounding box is a relevant approach in keeping the computation time as low as possible in a mesh free solutions since the solution time increases as the cell number. An alternative method to the bounding box method, is defining the integration cells manually up to a desired number of partitions in each axis so that total number of integration cells are controlled. The convergence behavior of manual method in the EFG approximation is illustrated in Fig. 9, for 5x5 node resolution and 7 Gauss points in each integration cell. Here, the coefficient of support domain was chosen as 2.05. Determination of the number of integration cells required to generate a sufficiently accurate solution is very important issue in the manual method, since a mesh free approximation may diverge from an accurate solution even with increased number of integration cells employed in the solution domain. In the numerical integration with manual method desired number of integration cell structures can be defined. However, the shape functions may have values close to zero in some integration cell and because of this poor numerical integration performance may occur. Hence, the numerical simulation results may cause some divergence from the correct solution of the problem.

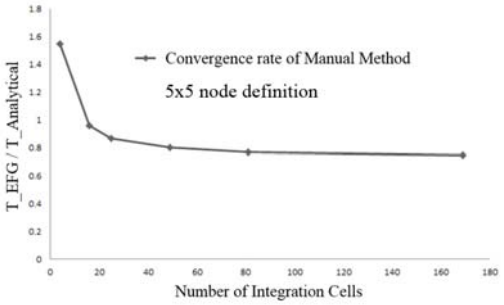


Fig. 9. Convergence behavior of Manual Method with the number of integration cells.

The numerical results obtained by employing both the bounding box and manual methods were compared in terms of the number of Gauss points defined within each integration cell as shown in Fig. 10. In these approximations a 9x9 node distribution defined in the solution domain and the same number of integration cells are created by using the bounding box and manual methods.

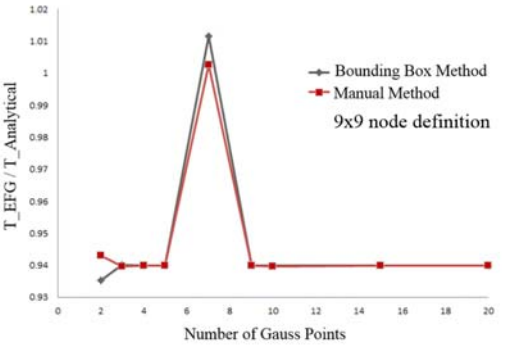


Fig. 10. Response of bounding box and manual method to number of integration points

The results show that models employing 3 to up to 20 Gauss integration points the model with just 7 Gauss integration points resulted in avery good approximation capturing almost the analytical solution for both the bounding box and manual methods. The geometry of the integration domains, so the Jacobian of the transformation, affect the performance of the numerical integration. Selection of a very small integration domains or if larger number of Gauss points are defined in an integration domain results in poor Jacobian which affects the accuracy of the approximation. For the considered problem, several numerical solutions were generated for different integration cells by using both the bounding box and manual methods. The aim here was to clarify the effects of the two choices, namely the employment of the bounding box and manual methods, in building the integrations cell structure for a predetermined node distribution. In each of these analyses, however, the distributions were different while the number of cells employed was constant. The results are shown in Fig. 11. As it is seen, at least

for the problem considered, the two methods give rise to almost the identical results.

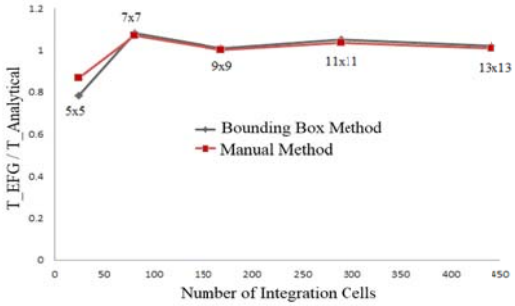


Fig. 11. Comparison of the results corresponding to the integration cell distributions generated by using the bounding box and manual methods

The numerical results presented in Figs. 9 and 11 show that the bounding box method has an advantage over the manual method that can even be applied in the initial approximation stages. As it is seen in Fig. 9, defining approximately 20 integration cells with manual method, results in the best approximation to the physical problem considered. However, increasing the number of integration domains gives rise to poor accuracy in numerical approximations. Therefore, in the manual method, the optimum number of integration domains cannot be predicted properly unless an initial approximation is present. The results presented in Fig. 11 were generated by using both the bounding box and manual methods in building the integration domains. The results depicted in Fig. 11, indicates that a very good approximation to analytical solution of the physical problem considered is obtained even in a large number of integration cell definition. In the rest of the paper, unless otherwise stated, the bounding box method was utilized in the construction of integration cell structures.

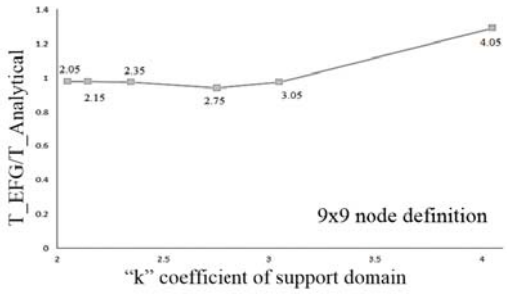


Fig. 12. Effect of support domain radius on EFG solution

The heat transfer problem defined in Fig. 3 was used to investigate the effects of the support domain radius for moving least squares shape functions. It is found that the support domain radius affects the performance of the EFG approximation. In order to predict the effect of support domain coefficient "k" on the performance of the EFG method, a 9x9 node distribution was defined in the solution domain and this node distribution was kept constant. In the analyses, in each of the integration cells 7 Gauss points were defined. A comparisons of the numerical solutions obtained for different k values with analytical predictions are shown in Fig. 12.

The values of support domain coefficient between 2 and 3 resulted in accurate approximations. In these analyses all the shape functions with linear polynomial basis were utilized and the results were obtained by applying the moving least squares approach with the spline type weight functions. For higher values of the support domain coefficient, the numerical predictions considerable diverge from the analytical solution. Hence, as a general definition to predict an appropriate support domain coefficient value for moving least squares shape functions, k, it should be between 2 and 3. The support domain coefficient controls the span of moving least squares shape functions. Because of that when the shape functions spread up to one third of the solution domain, the numerical solutions becomes almost identical to the analytical solution. In moving least squares approximation at least m+1 shape functions should intersect in the solution domain for an m_{th} order approximation. It is also important in the conversion of the moment matrix A(x) defined in Eq. 4, to obtain the moving least squares shape function explicitly.

To evaluate the effects of the support domain coefficient, k, on the EFG solution of the heat transfer problem, the analyses were repeated for four different k values. The results are summarised in Table 1. Here, the relative error is defined as $((T_{analytical}-T_{numerical})/T_{analytical})$.

k: coefficient of suppcrt domain	**k**=1.95	**k**=2.35	**k**=2.75	**k**=3.05
X: 5 nodes Y: 5 nodes Number of Integration Cells	*ri_x*=0.4875 *ri_y*=0.4875 Relative Error: 0.1062 49	*ri_x*=0.5875 *ri_y*=0.5875 Relative Error: 0.08731 25	*ri_x*=0.6875 *ri_y*=0.6875 Relative Error: 0.3088 25	*ri_x*=0.7625 *ri_y*=0.7625 Relative Error: 0.8145 9
X: 7 nodes Y: 5 nodes Number of Integration Cells	*ri_x*=0.3250 *ri_y*=0.4875 Relative Error: 0.07958 77	*ri_x*=0.391667 *ri_y*=0.587500 Relative Error: 0.0502 45	*ri_x*=0.45833 *ri_y*=0.68750 Relative Error: 0.2731 45	*ri_x*=0.50833 *ri_y*=0.76250 Relative Error: 0.7342 21
X: 7 nodes Y: 7 nodes Number of Integration Cells	*ri_x*=0.3250 *ri_y*=0.3250 Relative Error: 0.0543 121	*ri_x*=0.39167 *ri_y*=0.39167 Relative Error: 0.03987 81	*ri_x*=0.45833 *ri_y*=0.45833 Relative Error: 0.2211 81	*ri_x*=0.50833 *ri_y*=0.50833 Relative Error: 0.5871 69
X: 9 nodes Y: 9 nodes Number of Integration Cells	*ri_x*=0.24375 *ri_y*=0.24375 Relative Error: 0.02716 225	*ri_x*=0.29375 *ri_y*=0.29375 Relative Error: 0.02474 169	*ri_x*=0.34375 *ri_y*=0.34375 Relative Error: 0.1584 169	

Table 1. The EFG approximations with different support domain coefficients

In this Table, ri_x and ri_y are the support domain radii for x and y axes, respectively. Investigation of heat transfer problem was extended to include both a natural (or specified heat flux) and an essential (specified temperature) boundary conditions defined on the same solution domain. This new problem definition is shown in Fig. 13 [11].

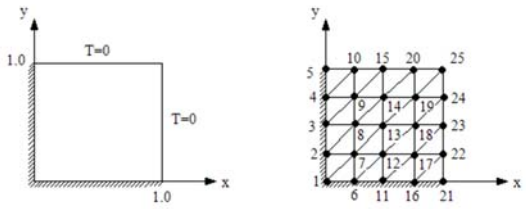


Fig. 13. Heat transfer problem with natural and essential boundary conditions and the FEM mesh.

The partial differential equation for the present heat transfer is given by Eq. 15

$$\frac{\partial T}{\partial t} - \left(\frac{\partial^2 T}{\partial x^2} + \frac{\partial^2 T}{\partial y^2}\right) = 1 \qquad (15)$$

For this problem, several approximate solutions were generated by utilizing a 5x5 node definition in the solution domain with various values of the coefficients on the support domain. For the numerical integration, 7 Gauss points are employed. In addition, for time integration Crank Nicholson time integration scheme is utilized. The comparison of the solutions obtained by using EFG and the FEM and the series solution [11] of the problem for t=1 are listed in Table 2.

Node Number	Analytical Solution	FEM (Steady)	EFG (5x5) k=1.75	EFG (5x5) k=1.35	EFG (5x5) k=1.25
1	0.2947	0.3013	0.2926	0.2941	0.2950
2	0.2789	0.2805	0.2774	0.2788	0.2795
3	0.2293	0.2292	0.2271	0.2295	0.2300
4	0.1397	0.1392	0.1405	0.1403	0.1404
6	0.2789	0.2805	0.2774	0.2788	0.2795
7	0.2642	0.2645	0.2629	0.2646	0.2651
8	0.2178	0.2172	0.2161	0.2183	0.2188
9	0.1333	0.1327	0.1329	0.1342	0.1342
11	0.2293	0.2292	0.2271	0.2295	0.2300
12	0.2178	0.2172	0.2161	0.2183	0.2188
13	0.1811	0.1801	0.1789	0.1819	0.1823
14	0.1127	0.1117	0.1123	0.1138	0.1139
16	0.1397	0.1392	0.1405	0.1403	0.1404
17	0.1333	0.1327	0.1329	0.1342	0.1342
18	0.1127	0.1117	0.1123	0.1138	0.1139
19	0.0728	0.0715	0.0737	0.0746	0.0747

Table 2. Comparison of the Analytical, EFG and FEM solutions of the heat transfer problem.

Relative error plots of EFG and FEM approximations in Table 2 depicted in Fig 14.

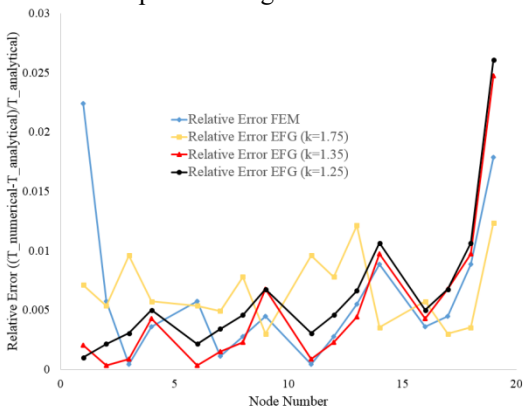


Fig. 14. Relative Error plots of EFG and FEM approximations

As it is seen, the results with the EFG method are compatible with the finite element and analytical solutions. The support domain of the meshless shape functions with k=1,35 where radius approaches to one third of the axis length, performs well for this heat transfer problem.

The third problem investigated by using the EFG Methods is a membrane vibration problem. Here, a square membrane having a unit length in both x and y directions, is considered. The solutions were generated for 7x5 and 11x7 node resolutions. The support domain coefficient for this problem is considered as to be 3.05. Partial differential equation for this physical problem is defined in Eq. 16. In Eq. 16, c=F/ρ, F being tension force applied on membrane and ρ the density of membrane material.

$$\frac{\partial^2 u}{\partial t^2} = c^2\left(\frac{\partial^2 u}{\partial x^2} + \frac{\partial^2 u}{\partial y^2}\right) \qquad (16)$$

Considering unit tension and unit density, analytical solution to the membrane vibration problem is given by Eq. 17 [10, 12]. The initial condition for the transverse deflection of the membrane is considered as u (x, y,0) =x(x-1) y(y-1) and membrane is released with zero initial speed.

$$\sum_{k=1}^{\infty}\sum_{l=1}^{\infty}\frac{64}{\pi^6(2k+1)^2(2l+1)^2}\sin\big((2k+1)\pi x\big)\sin\big((2l+1)\pi y\big)x\cos\big(\sqrt{(2k+1)^2+(2l+1)}t\big) \qquad (17)$$

The analytical solution to the transverse deflection of the membrane problem at t=2.04 seconds is illustrated in Fig. 15.

The EFG solutions for a 11x7 node resolution are illustrated in Figs. 16and17. In the EFG solution Newmark time integration scheme is employed.

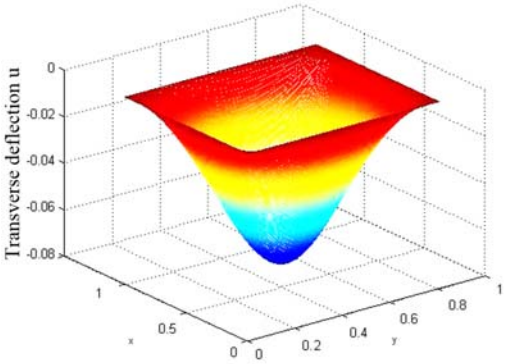


Fig. 15. Analytical solution of the transverse deflection of the membrane

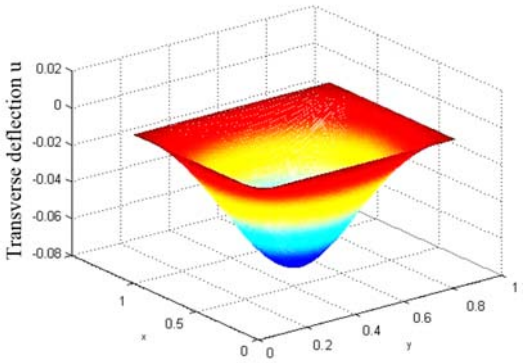


Fig. 16. The EFG solution of transverse deflection of a membrane problem at t=2.04 s with 11x7 node resolution.

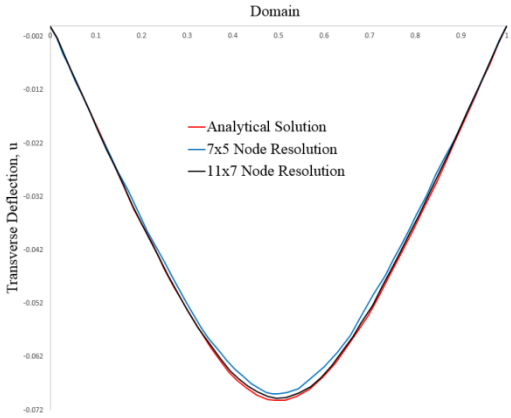


Fig. 17. The comparison of analytical and the EFG solutions with 7x5 and 11x7 node resolutions along the centerline (y=0.5) of transverse deflections for the membrane

As it is seen, for this problem the support domain coefficient of 3.05 resulted in a very satisfactory prediction of the transverse deflection of membrane.

IV. CONCLUSIONS

In the first part of this study, an approximation based upon the EFG meshless method and moving least squares interpolants were briefly reviewed. Then, in order to satisfy the Kronecker delta property, moving least squares (MLS) interpolants were modified. This transformation eases the enforcement of the essential (Dirichlet) boundary conditions as in the case they applied in FEM analyses. This makes meshless methods a strong alternative to FEM. Using the same numerical procedure with FEM, the meshless methods can easily be embedded in commercially available FEM software by making a number of small changes in the shape function construction.

The numerical integration procedure was described with the bounding box and the manual methods to define numerical integration cells (domains). The efficiencies of the both methods were investigated by considering a 2D heat transfer problem and the results were compared with the analytical solutions. The results indicate that the bounding box method with the spline type weight functions is more reliable than manually defining the integration domains. In addition, in the bounding box method no prior knowledge on the required number of integration cells for a well posed numerical simulation is necessary. This ease the necessity of the presence of a qualified person in the pre-processing stage of the numerical simulation in the meshless methods.

The effect of the value of the support domain radius on MLS shape functions constructed with the spline type weight functions were investigated by considering a transient heat transfer problems, and a transverse deflection of membrane problem.

In the solutions of all considered problems a support domain coefficient between 2 and 3 are well suited. It is also found that the optimum values for first order shape functions which were created by utilizing the spline type weight functions should spread to one third of the solution domain for an accurate solution. In addition to that, compact behavior of the shape functions should also be preserved.

In the numerical solution procedure, as it is usually the case the finite element method, increasing the number of shape functions employed in the EFG meshless approximations give rise to almost identical solutions to those obtained from the analytical solution of the physical problems studied.

REFERENCES

[1] Nayroles B., Touzot G., Villon P., Generalizing the Finite Element Method: Diffuse Approximation and Diffuse Elements. Comput. Mech., 10, 307 – 318, 1992.

[2] Fries T.P. and Matthies H.G., Classification and Overview of Meshfree Methods, http://bib1lp1.rz.tubs.de/docportal/servlets/MCRFileNodeServlet/DocPortal_derivate_00001418/Document.pdf;jsessionid=0000sSLpGS9lHECA1O-3HdgGFvt?hosts=local, spring, 2004.

[3] Belytschko T., Lu Y.Y., Gu L., Element-free Galerkin Methods. Internat. J. Numer. Methods Engrg., 37, 229 – 256, 1994.

[4] Dolbow J. and Belytschko T., Numerical Integration of Galerkin Weak Form in Meshfree Methods, Computational Mechanics, 23, 219-230, 1999.

[5] Liu G.R., Meshfree Methods: Moving Beyond The Finite Element Method, CRC Pres, 2003.

[6] Xiang X., Element Free Galerkin Method in Structural Mechanics, PhD. Thesis, Arlington, 1997.
[7] Atluri S.N., Kim H.G. and Cho Y.J., A Critical Assessment of The Truly Meshless Local Petrov-Galerkin (MLPG) and Local Boundary Integral Equation (LBIE) Methods, Computational Mechanics, 24, 348-372, 1999.
[8] Lancaster P. and Salkauskas K., Surfaces Generated by Moving Least Squares, Mathematics of Computation, 37, 155, 141-158, 1981.
[9] Raju I.S. and Phillips D.R., A Local Coordinate Approach in the MLPG Method forthe Beam Problems, Langley Research Center, Hampton, Paper No: NASA/TM 2002-211463, Virginia, 2002.
[10] Pala Y., Modern Uygulamalı Diferansiyel Denklemler, Nobel Yayın, First Edition, 2006.
[11] Reddy J.N., An Introduction to The Finite Element Method, Second Edition, McGraw-Hill International Editions, Singapore, 1993.
[12] Kreyszig E., Advanced Engineering Mathematics, Tenth Edition, John Wiley& Sons Inc., 2011.

★★★